Journal of Power Sources 223 (2013) 284–288

Contents lists available at SciVerse ScienceDirect

Journal of Power Sources

journal homepage: www.elsevier.com/locate/jpowsour

Short communication

# $Na_3V_2(PO_4)_3$ as cathode material for hybrid lithium ion batteries

Ke Du, Hongwei Guo, Guorong Hu, Zhongdong Peng, Yanbing Cao*

*School of Metallurgical Science and Engineering, Central South University, 932 Lushan South Road, Changsha 410083, China*

## HIGHLIGHTS

- We used the $Na_3V_2(PO_4)_3$ material as cathode material for hybrid lithium ion batteries for the first time.
- We introduced a mechanochemical activation assisted solid state carbothermal reduction reaction to synthesis the material.
- The product exhibited excellent cycling stability and rate performance in the hybrid ion system.
- Higher voltage plateau was exhibited than that in sodium ion batteries.

## ARTICLE INFO

*Article history:*
Received 17 May 2012
Received in revised form
6 August 2012
Accepted 13 September 2012
Available online 26 September 2012

*Keywords:*
Sodium super ion conductor
Hybrid lithium ion battery
Cathode material
Carbothermal reduction reaction

## ABSTRACT

$Na_3V_2(PO_4)_3$ of the rhombohedral NASICON structure has been prepared via solid state carbothermal reduction reaction assisted by mechanochemical activation. As a cathode material for hybrid lithium ion batteries, $Na_3V_2(PO_4)_3$ exhibits an initial specific discharge capacity of 114.2 mAh $g^{-1}$ in the voltage range between 2.5 V and 4.6 V, with a long discharge plateau near 3.7 V versus lithium metal. Approximately 3% of the discharge specific capacity is lost over the first 3 cycles at a current rate of 0.1 C. Then, the capacity appears to stabilize with the discharge specific capacity retention of 97.4% over the following 97 cycles. The material also exhibits good rate performance. Reversible capacities of 107.0 mAh $g^{-1}$ at a 1 C rate, 100.5 mAh $g^{-1}$ at 5 C and 84.4 mAh $g^{-1}$ at 10 C have been obtained. The preliminary results prove that $Na_3V_2(PO_4)_3$ is a new promising material for hybrid lithium ion batteries.



## 1. Introduction

NASICON (sodium super ion conductor)-related compounds, for instance, $Li_3V_2(PO_4)_3$ [1–4], $Li_2NaV_2(PO_4)_3$ [5] and $Li_3Ti_2(PO_4)_3$ [6], have been proved to be promising cathode materials for lithium-ion batteries, exhibiting high ion mobility and reasonable discharge capacity. In these NASICON-related compounds, lithium is essential as ion conductor. However, if other alkali metal containing material could work as cathode in lithium ion battery system, it will be significant for the developing of secondary batteries. The non-lithium containing cathode material $Na_3V_2(PO_4)_2F_3$ was a successful case that used as cathode material in a steady hybrid lithium ion battery system [7].

The non-lithium containing material $Na_3V_2(PO_4)_3$ was NASICON structured [8] and formerly used as electrode for sodium ion battery [9] or mid-product to obtain rhombohedral NASICON structured $Li_3V_2(PO_4)_3$ via ion exchanging [5,10,11]. In this work, $Na_3V_2(PO_4)_3$ was applied directly as cathode material to compose a so-called hybrid ion battery with lithium anode and lithium-containing electrolyte. An electro-catalysis [12,13] ion exchange reaction occurred on the cathode/electrolyte interface when the battery was working. The theoretical capacity is 176 mAh $g^{-1}$ based on all of the three $Na^+$ ions extracted from the material lattice. However, extraction of the third $Na^+$ (or $Li^+$) ion is kinetically difficult due to the much lower electronic/ionic conductivity of the end-member of $V_2(PO_4)_3$. Therefore, two-thirds of the $Na^+$ (or $Li^+$) ions which can be reversibly extracted/inserted give rise to a theoretical capacity of 118 mAh $g^{-1}$ [5,14]. We found that, in this hybrid ion system, the non-lithium containing NASICON-related material, $Na_3V_2(PO_4)_3$, showed excellent electrochemical performance.

## 2. Experimental

$Na_3V_2(PO_4)_3$ was prepared via solid state carbothermal reduction reaction (CTR) assisted by mechanochemical activation. $Na_2CO_3$, $NH_4H_2PO_4$, $V_2O_5$ and glucose were reacted in stoichiometric proportion at 600–800 °C in argon atmosphere for 12 h after a preliminary heating treatment of the mixture at 400 °C for 6 h. In

* Corresponding author. Tel.: +86 13387426652; fax: +86 (0)731 88876454.
*E-mail address:* ghw8people@126.com (Y. Cao).

0378-7753/$ – see front matter © 2012 Elsevier B.V. All rights reserved.
http://dx.doi.org/10.1016/j.jpowsour.2012.09.069

order to make the V (V) completely reduced to V (III), 35 wt.% extra glucose was added.

The crystallographic structure and phase analysis were provided from X-ray powder diffraction (XRD, D/max-r A type Cu $K_\alpha$). JADE software program was used to determine peak locations and intensities. The particle morphology of the products was observed by means of scanning electron microscopy (SEM, JEOL JSM-6360LV). The thermogravimetric analysis (TGA/DSC) of the samples was obtained using a Diamond TG thermo-analyzer. The concentration of sodium, lithium, vanadium and phosphorous of the samples was measured by inductively coupled plasma atomic emission spectroscopy (ICP-AES, Optima 4300DV).

To test the electrochemical performances, the cathode slurry (80 wt.% of the active material) was coated onto an aluminum foil followed by drying in vacuum at 120 °C for 12 h. The cells (CR2025) were assembled and disassembled in an argon filled glove-box using lithium metal foil as the anode. The electrolyte was 1.0 mol $L^{-1}$ $LiPF_6$ in a mixture of ethyl carbonate (EC), diethyl carbonate (DEC) and dimethyl carbonate (DMC) (volume ratio 1:1:1). The cathode films removed from the cells were washed by DMC. The cells were charged and discharged at 0.1 C in the voltage range of 2.5 V–4.6 V on charge/discharge apparatus (Land-BTL10) (Note that 0.1 C refers to two Na extraction from the $Na_3V_2(PO_4)_3$ per formula unit in 10 h.). Electrochemical impedance spectroscopy (EIS) and cyclic voltammetry (CV) were conducted by using an electrochemical working station (CHI660D). The amplitude is 5 mV and the frequency ranges between $1 \times 10^5$ and $1 \times 10^{-2}$ Hz for the EIS. The scan rate is 0.05 mV $s^{-1}$ and the voltage ranges between 2.5 V and 4.6 V for the CV.

## 3. Results and discussion

The TGA–DSC curves of the $Na_3V_2(PO_4)_3$ precursor ($V_2O_5$ + $NH_4H_2PO_4$ + $Na_2CO_3$ + glucose) are shown in Fig. 1(a). According to the DSC curve, the sharp endothermic peak between 100 °C and 200 °C is mainly caused by the evaporation of water, carbon dioxide and ammonia from the precursor. The endothermic effects between 300 °C and 600 °C are attributed to the decomposition of the glucose (between 300 °C and 400 °C) and the reduction of vanadium from V (V) to V (III) (between 500 °C and 600 °C). The sharp exothermic effect between 650 °C and 700 °C corresponds to the formation of the $Na_3V_2(PO_4)_3$ phase. The TG curve becomes flat above 750 °C, indicating the completion of the entire reaction. Fig. 1(b) presents the TG curve of the $Na_3V_2(PO_4)_3$/C sample under air atmosphere. Accordingly, the carbon content is 1.8 wt.%.

Fig. 2 shows the X-ray diffraction (XRD) pattern of the material, as well as the Rietveld refinement of the pattern. The figures of merit were $R_p$ = 8.29%, $wR_p$ = 12.79%, $\chi^2$ = 2.31. The diffraction peaks is in good agreement with previous reports [5,8]. According to the Rietveld refinement, the structural parameters are $a$ = 8.7241 Å and $c$ = 21.8239 Å indexed in the space group *R-3c* (*167*). The $Na^+$ ions occupy two sites in the structure, which is shown in Table 1. The characteristic diffraction peaks of crystallized graphite carbon are not observed from the XRD pattern. This provides evidence that residual carbon in the material is in amorphous state. The morphology of the material was studied by SEM as shown in Fig. 3. It can be seen that the irregularly shaped particles are distributed in the range of 1–5 μm due to the mechanochemical activation before sintering. Some of the particles are agglomerated to form larger secondary particles.

Fig. 4 displays the CV curves of the first three cycles for the material in the potential window of 2.5–4.6 V vs. $Li^+$/Li at a scan rate of 0.05 mV $s^{-1}$. The curves are composed of two redox couples, which can be assigned to the $V^{3+}/V^{4+}$ redox reaction accompanied

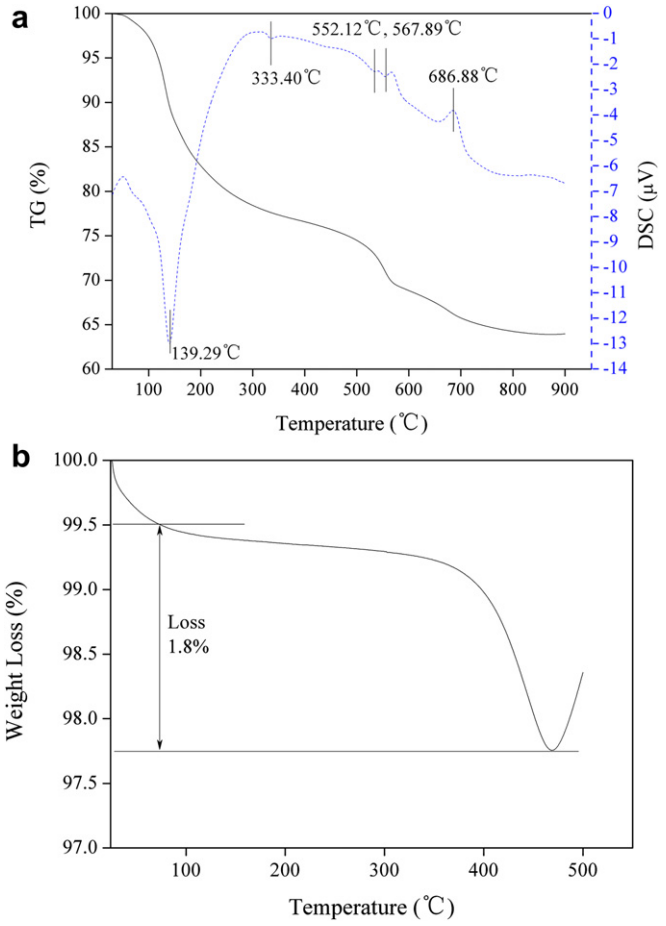


**Fig. 1.** (a) TGA–DSC curves of the $Na_3V_2(PO_4)_3$ precursor ($V_2O_5$ + $NH_4H_2PO_4$ + $Na_2CO_3$ + glucose) in argon atmosphere; (b) TGA curve of the $Na_3V_2(PO_4)_3$/C sample in air atmosphere.

by the extraction/insertion of two hybrid ions ($Na^+$ or $Li^+$) in the A (2) site of the NASICON structure [5,8]. The oxidation and reduction peaks are located closely at 3.85 V, 3.75 V and 3.70 V, 3.60 V, respectively. It is different from the result reported in Ref. [9], in which just one sharp redox couple was observed at 3.4 V vs. $Na^+$/Na in this voltage range. As the cycle progresses, the curves exhibit excellent symmetry, indicating good reversibility of the material.

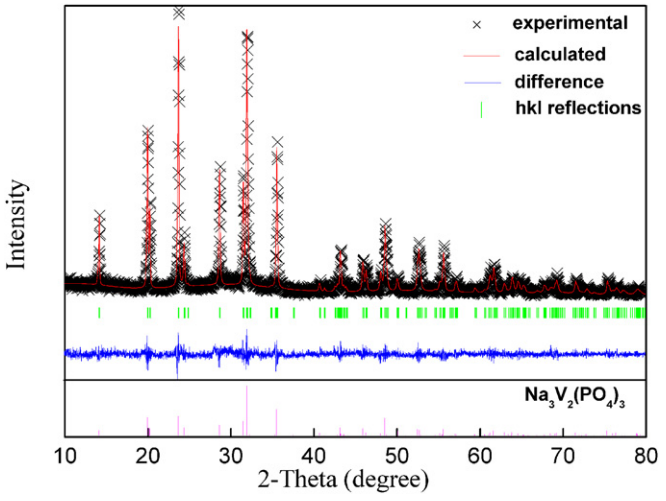


**Fig. 2.** XRD pattern of the material.

**Table 1**
Fractional atomic coordinates and isotropic displacement factors (Å$^2$).

| | *x* | *y* | *z* | $U_{iso}$ | Occ. |
|---|---|---|---|---|---|
| Na(1) | 0.333330 | 0.666670 | 0.166670 | 0.14397 | 0.8711 |
| Na(2) | 0.6666670 | 0.971206 | 0.0833330 | 0.06162 | 0.7001 |

To investigate the possibility of ion-exchange taking place between the $Na_3V_2(PO_4)_3$ and $Li^+$ electrolyte phase, the elements contents of the $Na_3V_2(PO_4)_3$ at different stages are analyzed by ICP-AES, which are listed in Table 2. S1 is the as-prepared powder sample and S2 is from the positive electrode of the assembled cell that has stood by for 4 h; S3 and S4 represent the sample after the first and tenth charge/discharge cycle. According to the ICP analysis, Li was found in the samples after contacting with electrolyte for 4 h and after charge/discharge cycle. It can be found that appreciable ion-exchange takes place after standing by 4 h for freshly assembled cells (S2), which means that $Na^+$ ions exchanged by $Li^+$ ions may occur before the charge/discharge cycles. With the further cycling, $Li^+$ ions replace nearly two-thirds of all the $Na^+$ ions in the material. It may be attributed to a gradual shift in the insertion mechanism from predominant $Na^+$ insertion to $Li^+$ insertion [15–17].

Fig. 5(a) presents the Nyquist plots of the composite. The impedance spectrum was fitted with the fitting equivalent circuit as shown in Fig. 5(b). According to Refs. [10,18], $R_e$ represents the solution resistance, $R_{ct}$ corresponds to the charge transfer resistance. $Z_w$ is related to the solid-state diffusion of ions in the active materials corresponding to the slopping line at the low frequency. $Q_{ct}$ is associated with the surface property of the electrode. $C_{int}$ signify the capacitance caused by ion transfer in the active material. The fitting results are shown in Table 3. All the errors are within bounds. Because the material was working in a hybrid ion system, the ion diffusion involves hybrid transferring of $Na^+/Li^+$. The ion diffusion coefficient is roughly estimated by using Eq. (1) [1,10] within our knowledge.

$$D = \frac{0.5R^2T^2}{S^2n^4F^4C^2\sigma^2} \quad (1)$$

In this equation, $R$ is the gas constant, $T$ is the absolute temperature, $F$ is the Faraday constant; $S$ is the active surface area [19,20] of the electrode which is 1.6 cm$^2$ in this work (Note that the total Brunauer–Emmett–Teller (BET) surface area $A_{BET} = 5.2$ m$^2$ g$^{-1}$); $n$ is the number of electrons per species reaction; $C$ is the concentration of $Na^+$ in the cathode electrode which is approximately

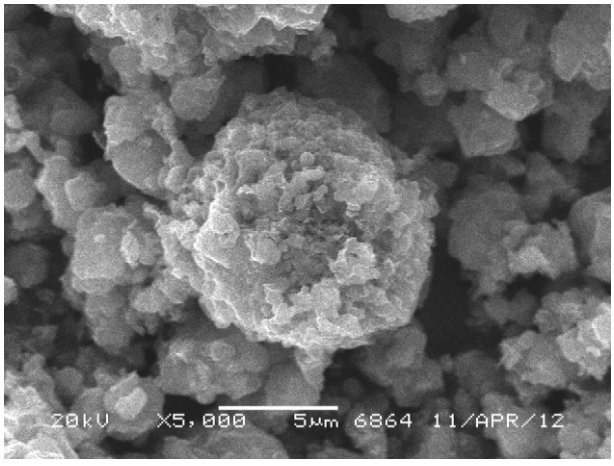


**Fig. 3.** SEM image of the material.

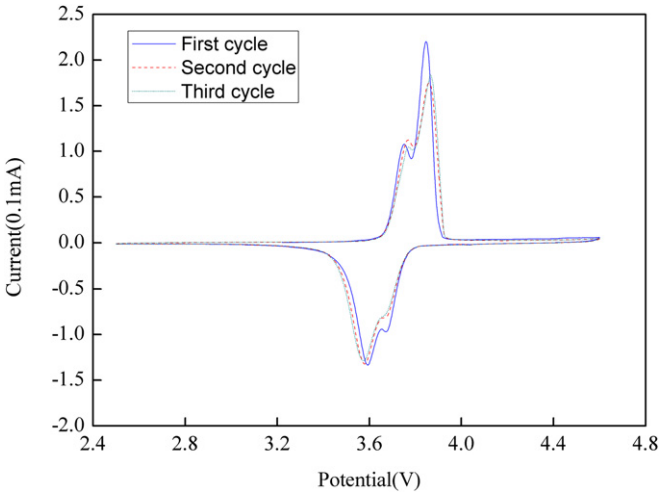


**Fig. 4.** CV curves of the material at 0.05 mV s$^{-1}$ in a voltage range of 2.5 V–4.6 V vs. $Li^+/Li$ over first three cycles.

$6.92 \times 10^{-3}$ mol cm$^{-3}$ as the chemical composition of the active material is $Na_3V_2(PO_4)_3$ (Note that the density is 3.156 g cm$^{-3}$ by Ref. [8]); $\sigma$ is the Warburg factor which obeys Eq. (2) [1,15].

$$Z' = R_e + R_{ct} + \sigma\omega^{-1/2} \quad (2)$$

Fig. 5(c) displays the linear fitting of Z′ vs. $\omega^{-1/2}$, from which the slope $\sigma$ 35.8 S$^{-1}$ s$^{-1/2}$ can be obtained. The result of the ion diffusion coefficient calculated using the two equations above is $2.23 \times 10^{-13}$ cm$^2$ s$^{-1}$.

Fig. 6(a) shows the charge/discharge curves of the first three cycles for the $Na_3V_2(PO_4)_3$/Li cells at a current rate of 0.1 C in the voltage range of 2.5–4.6 V. Two voltage plateaus approximately near 3.70 V and 3.80 V in the charge curves were observed. For the discharge curves, one voltage plateau near 3.65 V was observed and the other near 3.55 V was not that obvious. The charge/discharge curves correspond to the CV curves well. The voltage plateau of the material in this hybrid ion battery system is generally higher than that in the sodium ion battery system, which is 3.40 V reported by Jian et al. [9]. It is also higher than that of the traditional $LiFePO_4$ material, which is approximate 3.40 V reported previously [21,22]. Fig. 6(b) displays the initial charge/discharge curves at different current rates. The cells were charged/discharged at a 0.1 C rate over the first one hundred cycles and at a 0.5 C rate over the following five cycles; then over the next cycles, charged at 1 C and discharged respectively at 1 C, 2 C, 5 C and 10 C; finally charged/discharged back to 0.1 C over the last five cycles. The corresponding data of initial discharge capacities are listed in Table 4. It indicates an excellent rate performance of the material with the discharge specific capacity retention of 73.9% while the current rates rise up from 0.1 C to 10 C. Fig. 6(c) displays the discharge specific capacity vs. cycle numbers of the material at different current rates. Approximately 3% of the discharge specific capacity is lost over the

**Table 2**
The molar ratio of Na:Li:V:P of the samples at different stages.

| | The molar ratio of Na:Li:V:P | | | |
|---|---|---|---|---|
| | Li | Na | V | P |
| S1 | 0 | 3.081 | 2.033 | 3.024 |
| S2 | 1.378 | 1.571 | 2.071 | 3.082 |
| S3 | 1.735 | 1.253 | 2.012 | 3.037 |
| S4 | 2.026 | 1.015 | 2.042 | 3.041 |

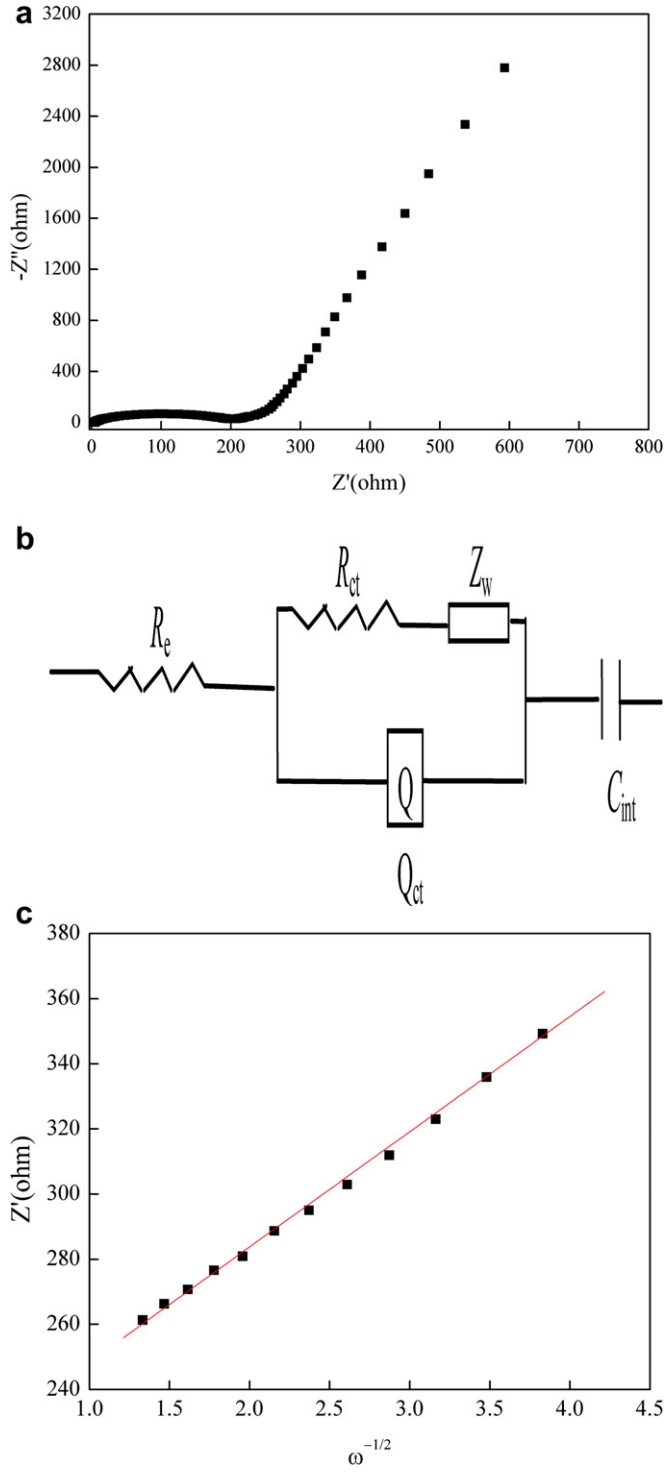


**Fig. 5.** (a) Nyquist plots of the material; (b) equivalent circuit model used for EIS fitting of the electrode; (c) linear fitting of $Z'$ vs. $\omega^{-1/2}$.

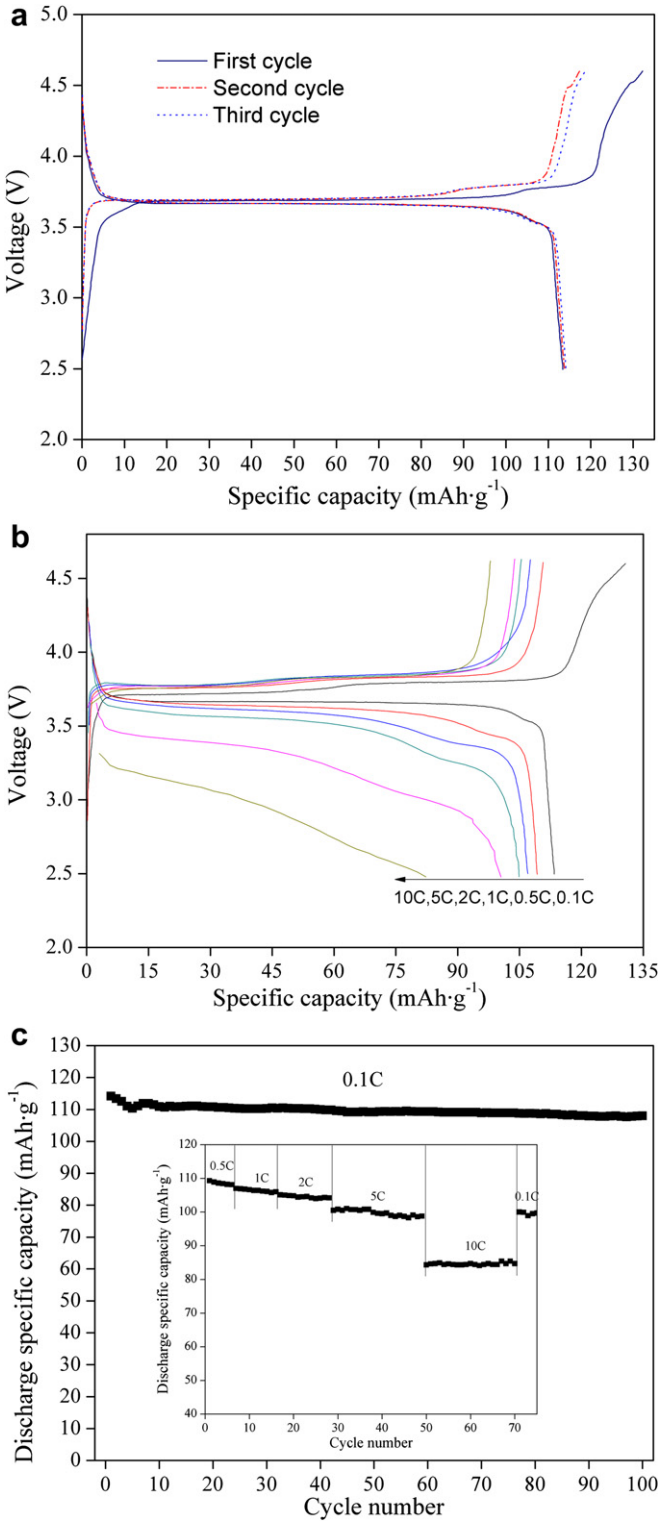


**Fig. 6.** (a) Charge/discharge curves of the first three cycles for the material at a current rate of 0.1 C in the voltage range of 2.5–4.6 V vs. $Li^+$/Li. (b) The initial charge/discharge curves at different current rate. (c) The discharge specific capacity vs. cycle numbers of the material at different current rate.

**Table 3**
Impedance parameters of the fitting equivalent circuit.

| | $R_e$(Ω cm$^{-2}$) | $R_{ct}$(Ω cm$^{-2}$) | $Z_w$(S s$^{1/2}$ cm$^{-2}$) | $Q_{ct}$(S s$^n$ cm$^{-2}$) | $C_{int}$(F cm$^{-2}$) |
|---|---|---|---|---|---|
| Results | 3.503 | 178.3 | 6.115E$^{-3}$ | 8.659E$^{-6}$ | 3.886E$^{-3}$ |
| Error(%) | 2.877 | 1.163 | 4.287 | 6.03 | 1.844 |

first 3 cycles at a 0.1 C rate, after which the capacity appears to stabilize. The discharge capacity retention is 97.4% over the following 97 cycles. At the high current rates, cycling stability is also exhibited, indicating that the $Na^+$ in this system wouldn't destroy this stability. The discharge specific capacity go averagely back to

**Table 4**
Initial discharge specific capacities of the material at different current rate.

| Specific capacity (mAh $g^{-1}$) | Current rate | | | | | |
|---|---|---|---|---|---|---|
| | 0.1 C | 0.5 C | 1 C | 2 C | 5 C | 10 C |
| Charge | 131.3 | 112.1 | 108.5 | 105.1 | 104.3 | 84.7 |
| Discharge | 114.2 | 109.3 | 107.0 | 104.9 | 100.5 | 84.4 |

100.9 mAh $g^{-1}$ while the discharge rate returns to 0.1 C from 10 C, which indicates that the crystal structure of the materials keeps well under higher discharge current.

## 4. Conclusion

The cathode material of the rhombohedral NASICON structure, $Na_3V_2(PO_4)_3$, is introduced for hybrid lithium ion batteries. It shows an initial reversible capacity of 114.2 mAh $g^{-1}$ at 0.1 C, with one obvious voltage plateaus near 3.70 V. Excellent cycling stability is exhibited at 0.1 C, which indicates that the $Na^+$ wouldn't destroy the stability in this system. The material also features good rate performance. Further work on the exact clarification of the electrochemical mechanism of this hybrid ion system and the optimization of the material will be carried out in the future.

## References

[1] T. Jiang, W. Pan, J. Wang, X. Bie, F. Du, Y. Wei, C. Wang, G. Chen, Electrochim. Acta 55 (2010) 3864–3869.
[2] A. Pan, D. Choi, J.G. Zhang, S. Liang, G. Cao, Z. Nie, B.W. Arey, J. Liu, J. Power Sources 196 (2011) 3646–3649.
[3] E. Kobayashi, L.S. Plashnitsa, T. Doi, S. Okada, J. Yamaki, Electrochem. Commun. 12 (2010) 894–896.
[4] J. Gaubicher, C. Wurm, G. Goward, C. Masquelier, L. Nazar, Chem. Mater. 12 (2000) 3240–3242.
[5] B.L. Cushing, J.B. Goodenough, J. Solid State Chem. 162 (2001) 176–181.
[6] H. Ohkawa, K. Yoshida, M. Saito, K. Uematsu, K. Toda, M. Sato, Chem. Lett. 10 (1999) 1017.
[7] J. Barker, R.K.B. Gover, P. Burns, A.J. Bryan, Electrochem. Solid State Lett. 9 (2006) A190–A192.
[8] I.V. Zatovsky, Acta Cryst. E66 (2010) i12.
[9] Z. Jian, L. Zhao, H. Pan, Y.S. Hu, H. Li, W. Chen, L. Chen, Electrochem. Commun. 14 (2012) 86–89.
[10] K.R. Franklin, E. Lee, J. Mater. Chem. 6 (l) (1996) 109–115.
[11] P.G. Bruce, A.R. Armstrong, R.L. Gitzendanner, J. Mater. Chem. 9 (1999) 193–198.
[12] S. Griese, D.K. Kampouris, R.O. Kadara, C.E. Banks, Electrochem. Commun. 10 (2008) 1633–1635.
[13] V.R. Chaudhari, M.A. Bhat, P.P. Ingole, S.K. Hanram, Electrochem. Commun. 11 (2009) 994–996.
[14] S.C. Yin, H. Grondey, P. Strobel, M. Anne, L.F. Nazar, J. Am. Chem. Soc. 125 (2003) 10402–10411.
[15] T. Jiang, G. Chen, A. Li, C. Wang, Y. Wei, J. Alloys Compd. 478 (2009) 604–607.
[16] J. Zhao, J. He, X. Ding, J. Zhou, Y. Ma, S. Wu, R. Huang, J. Power Sources 195 (2010) 6854–6859.
[17] X.Z. Liao, Z.F. Ma, Q. Gong, Y.S. He, L. Pei, L.J. Zeng, Electrochem. Commun. 10 (2008) 691–694.
[18] J. Barker, M.Y. Saidi, J.L. Swoyer, J. Electrochem. Soc. 151 (10) (2004) A1670–A1677.
[19] D.Y.W. Yu, C. Fietzek, W. Weydanz, K. Donoue, T. Inoue, H. Kurokawa, S. Fujitani, J. Electrochem. Soc. 154 (4) (2007) A253–A257.
[20] F. Gao, Z.Y. Tang, Electrochim. Acta 53 (2008) 5071–5075.
[21] M. Yao, K. Okuno, T. Iwaki, M. Kato, S. Tanase, K. Emura, T. Sakai, J. Power Sources 1173 (2007) 545–549.
[22] C. Li, N. Hua, C. Wang, X. Kang, T. Wumair, Y. Han, J. Alloys Compd. 509 (2011) 1897–1900.